JACS
JOURNAL OF THE AMERICAN CHEMICAL SOCIETY
Article
pubs.acs.org/JACS

# Electronically Stabilized Nonplanar Phenalenyl Radical and Its Planar Isomer

Ommid Anamimoghadam, Mark D. Symes, De-Liang Long, Stephen Sproules, Leroy Cronin, and Götz Bucher*

WestChem, School of Chemistry, University of Glasgow, Glasgow G12 8QQ, United Kingdom

Supporting Information

**ABSTRACT:** Stable phenalenyl radicals have great potential as the basis for new materials for applications in the field of molecular electronics. In particular, electronically stabilized phenalenyl species that do not require steric shielding are molecules of fundamental interest, but are notoriously difficult to synthesize. Herein, the synthesis and characterization of two phenalenyl-type cations is reported: planar benzo[*i*]naphtho-[2,1,8-*mna*]xanthenium ($8^+$) and helical benzo[*a*]naphtho-[8,1,2-*jkl*]xanthenium ($9^+$), which can be reduced to the corresponding radicals. Radical **9** represents the first stable, helical phenalenyl radical which does not rely on bulky substituents to ensure its stability. Both cations are water-soluble, and the radicals are stable for weeks at room temperature under air. These compounds were characterized crystallographically, and also by NMR, EPR, electrochemistry, and electronic spectra. The synthesis of the previously reported compound benzo[5,6]-naphthaceno[1,12,11,10-*jklmna*]xanthylium ($5^+$), the largest oxygen-containing polycyclic hydrocarbon, was undertaken for comparison with $8^+$ and $9^+$, allowing us to report its crystal structure here for the first time. The different properties of these compounds and their radicals are explained by considering their differing aromaticities using in-depth computational methods.

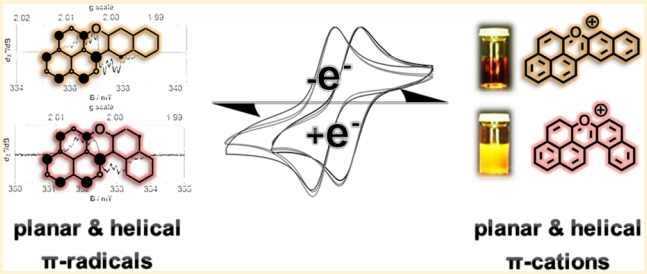


## INTRODUCTION

The quest to identify stable $\pi$-conjugated cations and radicals that do not require steric shielding has fascinated chemists for decades.[1−13] These compounds are of great fundamental interest, and yet they also have a range of potential applications in photochemistry,[14,15] synthesis,[16,17] materials science,[18−21] spintronics,[22−24] and biology.[25,26] In particular, open-shell polycyclic aromatic hydrocarbons have been shown to be promising molecular conductors and spin carriers in the emerging field of organic spin chemistry.[27]

On account of the reactivity of open-shell species, however, it is often necessary to strike a compromise between stability and functionality. For example, in spintronics applications, there must be excellent communication between spins, which means that relatively exposed radical centers are desirable;[2] however, this also favors radical dimerization and hence spin inactivation. Incorporation of bulky substituents to prevent dimerization can stabilize such radicals but also isolates the spins, reducing any desirable interactions.

An alternative strategy involves electronic stabilization through incorporation of heteroatoms into the polycyclic aromatic hydrocarbon to decrease the spin densities, eliminating the need for bulky groups.[28,29] However, this strategy may not always be favorable for the design of stable $\pi$-radicals, for the nature of the polycyclic framework and the position of the incorporated heteroatom(s) are critical for the spin distribution in the molecule. Hence, it is important to consider substructures that are conducive to efficient electronic stabilization such as the phenalenyl moiety, which affords good delocalization and spin-active $\pi$-dimerization.[30] Trioxatriangelenum ($1^+$) (see Figure 1) is a case in point: it is a remarkably stable pyrylium-based carbenium ion, but due to its polycyclic framework (which incorporates three oxygen atoms), the spin density when $1^+$ is reduced by one electron is weakly delocalized; i.e., the unpaired electron is not prone to distribute

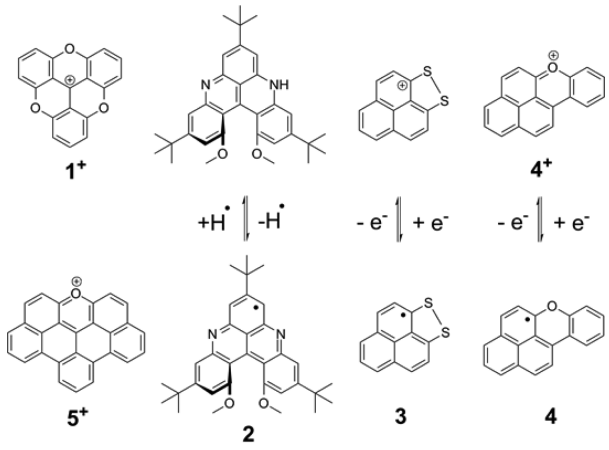


**Figure 1.** Molecular structures of $1^+$, **2**, **3**, $4^+$, **4**, and $5^+$.

**Received:** August 10, 2015
**Published:** November 2, 2015





DOI: 10.1021/jacs.5b07959
J. Am. Chem. Soc. 2015, 137, 14944−14951

across the phenyl rings. As a result, the one-electron reduction of $1^+$ does not result in stable open-shell species but in short-lived radicals that undergo rapid $\sigma$-dimerization between the central carbon atoms.[31,32] The first helical structural analogue of $1^+$ that can form a stable radical has recently been reported (compound **2**), wherein the radical is protected by sterically hindering groups.[33,34]

Pioneering work in this field has been performed by Haddon et al., leading to the synthesis of 1,9-dithiophenalenyl (**3**) stabilized via a disulfide bridge.[28,29] Meanwhile, our groups previously reported the first example of electronic stabilization by an oxygen atom in the phenalenyl species naphtho[2,1,8-*mna*]xanthenyl (**4**), which was generated by reduction of the parent cation.[35] Further planar stable open-shell species have been prepared by Kubo et al. which are stabilized through delocalization in a large polyaromatic framework. Also bulky substituents were introduced to obtain crystals for X-ray structure analysis.[36]

Herein, we describe the synthesis and characterization of two unprecedented phenalenyl species with intriguing properties (benzo[*i*]naphtho[2,1,8-*mna*]xanthenium ($8^+$) and benzo[*a*]-naphtho[8,1,2-*jkl*]xanthenium ($9^+$)), which we compare with $5^+$, the largest oxygen-incorporating polycyclic hydrocarbon.[37] Interestingly, while cation $8^+$ is planar, cation $9^+$ is helical. The radicals of both **8** and **9** could be produced on a preparative scale via bulk electrolysis of the corresponding solutions of the cations, and their properties were investigated by EPR spectroscopy and computational methods. Remarkably, the radicals can be stored under an air atmosphere for weeks, and both **8** and **9** show astonishingly stable redox behavior under air. To our knowledge, radical **9** represents the first electronically stabilized nonplanar phenalenyl-type radical without sterically hindering groups yet reported. Using EPR spectroscopy analysis supported by simulated spectra, we can confirm distinctly lower spin densities at the $\alpha$-positions of the phenalenyl skeletons of **8** and **9** compared with 1,9-dithiophenalenyl (**3**).[28,29] This decrease of the spin densities suggests a lower tendency for $\sigma$-dimerization of **8** and **9** compared to **3**.

In spite of their large size, both $8^+$ and $9^+$ are soluble in aqueous media (with the correct choice of counterion), which may serve to make them suitable as dyes or prospective DNA intercalators.[25] Crystal structures were obtained for both $8^+$ and $9^+$, and these cations exhibit interesting photochemical and redox behavior. We also prepared the previously reported cation of benzo[5,6]naphthaceno[1,12,11,10-*jklmna*]-xanthylium ($5^+$)—the largest polycyclic hydrocarbon containing a pyrylium moiety yet synthesized—to compare the differences in its structural and electronic properties with those of $8^+$ and $9^+$. Our investigations of $5^+$ have allowed us to obtain the crystal structure of this cation for the first time.

## EXPERIMENTAL SECTION

**General Procedure for the Synthesis of 9-(Methoxynaphthalenyl)-1*H*-phenalen-1-ones.** In a two-neck round-bottom flask, Mg in 5 mL of THF was activated with 0.1 mL of 1,2-dibromoethane under argon. Then the brominated aryl compound was added to the reaction mixture dropwise in THF by means of a syringe. With slow stirring and heating, the Grignard reagent began to form. After 45 min, 1.00 g (5.5 mmol, 1 equiv) of 1*H*-phenalen-1-one dissolved in 10 mL of dry THF was gradually added to the gray solution. The mixture was then refluxed for 4 h. After the mixture was cooled to room temperature, the reaction was quenched with 5 mL of satd $NH_4Cl$ solution. Then 20 mL of $H_2O$ was added, and the product was extracted with EtOAc (3 × 30 mL), washed with 20 mL of brine, and dried over $MgSO_4$. When the solvent was evaporated to dryness, the crude product and 1.30 g of DDQ (5.6 mmol, 1 equiv) were mixed in $CH_2Cl_2$ and refluxed overnight at 55−60 °C. The next day, the solvent was evaporated by rotary evaporator inside a fumehood. By flash column chromatography using silica and $CH_2Cl_2$ as the eluent, the desired product was obtained.

**Synthesis of 9-(3-Methoxynaphthalenyl)-1*H*-phenalen-1-one (6).** Following the general procedure, the Grignard reagent was generated from 0.23 g (9.4 mmol, 1.7 equiv) of Mg and 1.97 g (8.32 mmol, 1.5 equiv) of 2-bromo-3-methoxynaphthalene dissolved in 5 mL of THF at 40−50 °C. After reflux with 1*H*-phenalen-1-one (1 equiv) and subsequent oxidation with DDQ, 9-(3-methoxynaphthalenyl)-1*H*-phenalen-1-one was obtained as a yellow powder in a yield of 36% (0.68 g, 2 mmol). $^1$H NMR (400 MHz, $CDCl_3$): $\delta$ 3.79 (s, OMe), 6.58 (d, $J$ = 9.7 Hz, 1H), 7.22 (s, 1H), 7.33 (ddd, $J$ = 8.1, 6.9, 1.2 Hz, 1H), 7.44 (ddd, $J$ = 8.2, 6.9, 1.3 Hz, 1H), 7.64−7.60 (m, 2H), 7.66 (d, $J$ = 8.2 Hz, 1H), 7.69 (d, $J$ = 9.8 Hz, 1H), 7.77 (t, $J$ = 7.6 Hz, 1H), 7.80 (dd, $J$ = 8.2, 0.5 Hz, 1H), 8.06 (dd, $J$ = 8.2, 1.0 Hz, 1H), 8.22 (d, $J$ = 8.3 Hz, 1H). $^{13}$C NMR (100 MHz, $CDCl_3$): $\delta$ 55.78 (OMe), 105.49 (Cq), 123.73 (CH), 126.28 (CH), 126.24 (CH), 126.84 (CH), 127.47 (CH), 127.87 (2CH), 128.36 (Cq), 128.86 (Cq), 129.54 (Cq), 130.35 (CH), 131.20 (2CH), 131.73 (CH), 131.84 (CH), 132.28 (Cq), 133.94 (CH), 134.64 (Cq), 134.85 (Cq), 140.35 (Cq), 155.79 (Cq), 185.49 (C═O). UV (in MeCN): $\lambda_{max}$ [nm] (log $\varepsilon$) 305 (3.73), 320 (3.75), 360 (3.97). IR (ATIR): $\nu_{max}$ [$cm^{-1}$] 3010−2827 ($CH_{aromatic}$, weak), 1636 (C═O, sharp and intense), 1622, 1598, 1579, 1555, 1503, 1497, 1476, 1458, 1427, 1390, 1385, 1352, 1327, 1248, 1244, 1241 (C−O, sharp), 1198, 1171, 1123, 1107, 1076, 1040. MS (EI+): $m/z$ (relative intensity): 336 ($M^+$, 23), 320 (7), 306 (80), 305 (100), 292 (14), 276 (27), 263 (30), 237 (7), 160 (18), 153 (23), 146 (15), 132 (11), 86 (12), 84 (18), 49 (12), 44 (8). HRMS: calcd for $C_{24}H_{16}O$, 336.1150; found, 336.1146. Melting point: 194−196 °C (recrystallization from $CH_2Cl_2$).

**Synthesis of 9-(2-Methoxynaphthalenyl)-1*H*-phenalen-1-one (7).** Following the general procedure, the Grignard reagent was generated from 0.23 g (9.4 mmol, 1.7 equiv) of Mg and 1.97 g (8.32 mmol, 1.5 equiv) of 1-bromo-2-methoxynaphthalene dissolved in 5 mL of THF at 40−50 °C. After reflux with 1*H*-phenalen-1-one (1 equiv) and subsequent oxidation with DDQ, 9-(2-methoxynaphthalenyl)-1*H*-phenalen-1-one was obtained as an orange powder in a yield of 70% (1.30 g, 3.86 mmol). $^1$H NMR (400 MHz, $CDCl_3$): $\delta$ 3.79 (s, OMe), 6.50 (d, $J$ = 9.7 Hz, 1H), 7.10 (d, $J$ = 8.5 Hz, 1H), 7.20 (ddd, $J$ = 8.1, 6.7, 1.3 Hz, 1H), 7.30 (ddd, $J$ = 8.1, 6.7, 1.2 Hz, 1H), 7.42 (d, $J$ = 9.0 Hz, 1H), 7.59 (d, $J$ = 8.3 Hz, 1H), 7.66 (dd, $J$ = 8.2, 7.1 Hz, 1H), 7.70 (d, $J$ = 9.7 Hz, 1H), 7.80 (d, $J$ = 6.3 Hz, 1H), 7.85 (d, $J$ = 8.1 Hz, 1H), 7.94 (d, $J$ = 9.0 Hz, 1H), 8.10 (d, $J$ = 8.2 Hz, 1H), 8.27 (d, $J$ = 8.3 Hz, 1H). $^{13}$C NMR (100 MHz, $CDCl_3$): $\delta$ 56.85 (OMe), 77.36 (Cq), 113.95 (CH), 123.58 (CH), 124.16 (CH), 126.23 (Cq), 126.35 (CH), 126.54 (CH), 127.97 (Cq), 128.29 (CH), 128.66 (Cq), 128.70 (Cq), 128.94 (CH), 129.44 (Cq), 130.33 (CH), 131.15 (CH), 131.84 (CH), 132.20 (Cq), 132.56 (CH), 134.21 (CH), 140.41 (CH), 142.38 (Cq), 153.06 (Cq), 185.39 (C═O). UV (in MeCN): $\lambda_{max}$ [nm] (log $\varepsilon$) 312 (3.75), 341 (3.91), 358 (4.03). IR (ATIR): $\nu_{max}$ [$cm^{-1}$] 3032−2830 ($CH_{aromatic}$, weak), 1630 (C═O, sharp and intense), 1609, 1591, 1545, 1510, 1447, 1380, 1384, 1329, 1253 (C−O, sharp and intense), 1236, 1183, 1176, 1145, 1120, 1084, 1065, 1064. MS (EI+): $m/z$ (relative intensity) 336 ($M^+$, 9), 305 (93), 263 (7), 153 (8), 86 (65), 84 (100), 51 (22), 49 (68), 47 (18). HRMS: calcd for $C_{24}H_{16}O$, 336.1150; found, 336.1145. Melting point: 203−205 °C (recrystallization from $CH_2Cl_2$).

**General Procedure for the Synthesis of Benzonaphthoxanthenium Cations.** A 0.100 g sample of 9-(2-methoxyaryl)-1*H*-phenalen-1-one (0.35 mmol) was dissolved in 40 mL of $CH_2Cl_2$ in a round-bottom flask placed in a NaCl/ice bath. Argon was purged through for 5 min, and the flask was sealed with a septum and supplied with an argon-filled balloon. With stirring, 1.2 mL of $BBr_3$ in heptane (1 M) was slowly added by syringe. The color of the solution changed from orange to dark brown. After 10 min, the NaCl/ice bath was removed, and the solution was stirred for 4 h. After this time, adding


DOI: 10.1021/jacs.5b07959
J. Am. Chem. Soc. 2015, 137, 14944−14951

30 mL of $H_2O$ quenched the reaction and dissolved the precipitate, giving an orange solution. The aqueous layer was separated, and the organic salt in the organic layer was extracted with distilled $H_2O$ (2 × 10 mL). After the aqueous layers were combined and filtered, 5 mL of $HBF_4$ solution was added, yielding a precipitate which was separated by vacuum filtration.

**Synthesis of Benzo[*i*]naphtho[2,1,8-*mna*]xanthenium Tetrafluoroborate ($8^+$).** Following the general procedure, $8^+$ was obtained as a brown powder in a yield of 64%. $^1$H NMR (400 MHz, $CD_3CN$): $\delta$ 7.71 (t, $J$ = 7.5 Hz, 1H), 7.79 (t, $J$ = 7.1 Hz, 1H), 8.15 (d, $J$ = 8.4 Hz, 1H), 8.25 (d, $J$ = 8.5 Hz, 1H), 8.39 (d, $J$ = 9.1 Hz, 1H), 8.43 (t, $J$ = 7.7 Hz, 1H), 8.61 (s, 1H), 9.05 (m, 2H), 9.20 (d, $J$ = 8.7 Hz, 1H), 9.29 (d, $J$ = 9.1 Hz, 1H), 9.36 (d, $J$ = 8.7 Hz, 1H), 9.49 (s, 1H). $^{13}$C NMR (100 MHz, $CD_3CN$): $\delta$ 115.63 (Cq), 116.82 (CH), 118.66 (Cq), 120.92 (CH), 122.33 (Cq), 123.45 (CH), 128.40 (CH), 128.48 (CH), 128.63 (Cq), 128.96 (CH), 130.21 (CH), 131.20 (Cq), 131.45 (CH), 131.86 (CH), 132.33 (Cq), 137.30 (Cq), 141.83 (CH), 142.75 (CH), 145.96 (Cq), 148.40 (CH), 149.11 (Cq), 150.36 (CH), 166.07 (C═O$^+$). UV (in MeCN): $\lambda_{max}$ [nm] (log $\varepsilon$) 322 (4.15), 363 (3.82), 469 (4.68). IR (ATIR): $\nu_{max}$ [cm$^{-1}$] 3074 ($CH_{aromatic}$, weak), 1603, 1597, 1591, 1566 (C═O+, sharp and intense), 1507, 1472, 1445, 1421, 1360, 1334, 1288, 1239, 1211, 1199, 1163, 1144, 1136, 1027 (B−F, sharp and intense). MS (EI+): $m/z$ (relative intensity) 305 (100), 276 (21), 274 (9), 231 (5), 219 (5), 187 (8), 181 (7), 169 (8), 153 (13), 131 (10), 119 (8), 85 (6), 69 (16), 44 (83), 40 (15), 36 (22). HRMS: calcd for $C_{23}H_{13}O^+$, 305.0966; found, 336.0967. Melting point: 276−280 °C (recrystallization from acetone).

**Synthesis of Benzo[*a*]naphtho[8,1,2-*jkl*]xanthenium Tetrafluoroborate ($9^+$).** Following the general procedure, $9^+$ was obtained as a brown powder in a yield of 67%. $^1$H NMR (400 MHz, $CD_3CN$): $\delta$ 7.95 (ddd, $J$ = 8.0, 7.1, 1.0 Hz, 1H), 8.07 (ddd, $J$ = 8.5, 7.1, 1.4 Hz, 1H), 8.26 (d, $J$ = 9.1 Hz, 1H), 8.33 (dd, $J$ = 8.0, 1.2 Hz, 1H), 8.58 (t, $J$ = 7.7 Hz, 1H), 8.60 (d, $J$ = 9.1 Hz, 1H), 8.69 (d, $J$ = 9.1 Hz, 1H), 9.18−9.10 (m, 2H), 9.28 (d, $J$ = 8.5 Hz, 1H), 9.34 (d, $J$ = 9.1 Hz, 1H), 9.39 (d, $J$ = 9.1 Hz, 1H), 9.61 (d, $J$ = 9.1 Hz, 1H). $^{13}$C NMR (100 MHz, $CD_3CN$): $\delta$ 117.00 (Cq), 117.64 (Cq), 118.65 (CH), 120.11 (CH), 121.84 (Cq), 126.27 (CH), 128.26 (CH), 129.20 (Cq), 129.24 (Cq), 129.97 (CH), 130.57 (Cq), 131.39 (CH), 131.43 (CH), 131.45 (CH), 133.17 (Cq), 139.27 (CH), 140.42 (CH), 140.95 (CH), 144.32 (Cq), 146.73 (CH), 146.88 (CH), 155.76 (Cq), 161.38 (C═O$^+$). UV (in MeCN): $\lambda_{max}$ [nm] (log $\varepsilon$) 311 (4.91), 505 (5.12). IR (ATIR): $\nu_{max}$ [cm$^{-1}$] 3061, 1617, 1602, 1577, 1564, 1545, 1518, 1495, 1472, 1431, 1412, 1382, 1350, 1324, 1279, 1246, 1236, 1224, 1192, 1176, 1147, 1137, 1115, 1091, 1032, 983. MS (EI+): $m/z$ (relative intensity) 305 (100), 276 (28), 274 (10), 153 (9), 152 (8), 137 (7), 69 (3), 44 (4), 40 (3). HRMS: calcd for $C_{23}H_{13}O^+$, 305.0966; found, 305.0972. Melting point: 273−275 °C (recrystallization from acetone).

**Synthesis of Benzo[5,6]naphthaceno[1,12,11,10-*jklmna*]xanthylium Tetrafluoroborate ($5^+$).** In a two-neck round-bottom flask, 300 mg (0.8 mmol; 1 equiv) of 14-phenyl-14*H*-dibenzo[*a*,*j*]xanthene was dissolved in 25 mL of glacial acetic acid under reflux at 100 °C. Then 0.05 mL (1 mmol; 1.2 equiv) of $Br_2$ mixed with 5 mL of acetic acid was added dropwise to the solution, and the reaction was refluxed for 30 min. After the red solution was cooled, the precipitate was separated by vacuum filtration. The crude product was recrystallized from acetic acid, resulting in 14-phenyldibenzo[*a*,*j*]xanthenium bromide as red-orange crystals with a golden luster in a yield of 59% (216 mg, 0.5 mmol; lit.[37] yield 83%). Without further purification, the batch of 14-phenyldibenzo[*a*,*j*]xanthenium bromide was dissolved in 60 mL of MeCN and 5 mL of $HBF_4$ solution (48 wt % in $H_2O$). After UV irradiation overnight, black needles of $5^+$ were obtained in a yield of 30% over two steps (112 mg, 0.3 mmol). This compound was analyzed as per the analogous bromide salt previously reported.[37] IR (ATIR): $\nu_{max}$ [cm$^{-1}$] 3055 ($CH_{aromatics}$, weak), 1617, 1605, 1582 (C═O$^+$, intense), 1464, 1431, 1395, 1353, 1335, 1314, 1264, 1251, 1241, 1210, 1199, 1144, 1077, 1022 (B−F, intense). MS (FAB+) $m/z$ (relative intensity): 353 (36), 121 (30), 91 (10), 77 (10), 44 (100). Melting point: >360 °C (recrystallization from acetonitrile). HRMS: calcd for $C_{27}H_{13}O$, 353.0966; found, 353.0968.

**Computational Methods.** All calculations were performed using the Gaussian09 suite of programs.[38] Optimizations were performed using the B3LYP[39] and M05-2X[40] density functional methods, in combination with the 6-31G** and 6-31+G* basis sets.[41] All minima were characterized as such by performing a vibrational analysis.

## RESULTS AND DISCUSSION

Our synthetic methodology is shown in Scheme 1, and is based on a four-step synthesis via the two new precursors 9-(3-methoxynaphthalenyl)-1*H*-phenalen-1-one (**6**) (which gives $8^+$) and 9-(2-methoxynaphthalenyl)-1*H*-phenalen-1-one (**7**) (which leads to $9^+$).

**Scheme 1. Synthesis of Phenalenyl Cations and Radicals**[a]

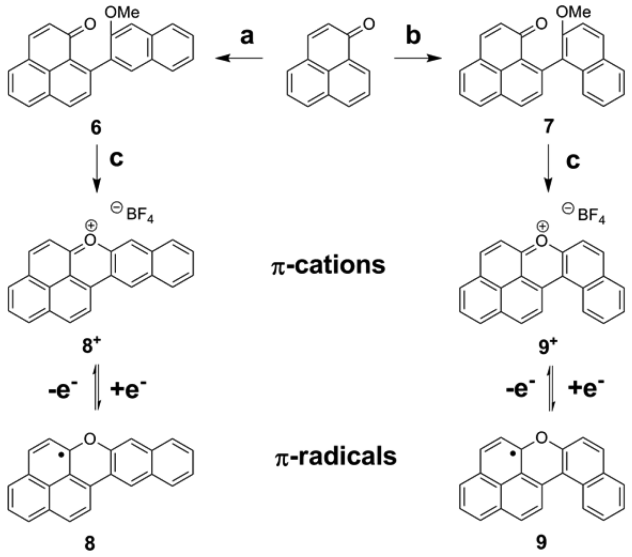


[a]Reagents and conditions: (a) (i) (3-methoxynaphthalen-2-yl) magnesium bromide, THF, rt; (ii) DDQ, $CH_2Cl_2$, reflux; (b) (i) (2-methoxynaphthalen-1-yl)magnesium bromide, THF, rt; (ii) DDQ, $CH_2Cl_2$, reflux; (c) (i) $BBr_3$, $CH_2Cl_2$, 0 °C to rt; (ii) $HBF_4$ (48 wt % in $H_2O$).

Both precursors were synthesized by a Michael-type Grignard addition to the 9-C position of 1*H*-phenalenone, with subsequent oxidation using DDQ.[42] This procedure gave **6** and **7** in yields of 36% and 70%, respectively, over two steps. Subsequently, demethylation using $BBr_3$ in $CH_2Cl_2$ resulted in the corresponding 9-(hydroxynaphthalenyl)-1*H*-phenalen-1-ones, which underwent rapid cyclization in the presence of water to give $8^+$ and $9^+$ with bromide as the counterion. These salts were soluble in water and were isolated in pure form by extraction into aqueous solution followed by precipitation as the tetrafluoroborate salts, yielding $8^+$ (64%) and $9^+$ (67%).

Cation $8^+$ crystallized from acetone in a triclinic system with space group $P\bar{1}$ (see Table S4 and Figure S6 in the Supporting Information). The molecules in this structure are arranged in $\pi-\pi$ stacking arrays separated by distances of between 3.286 and 3.389 Å. $8^+$ can be considered planar with a negligibly small torsion angle of 1.068° in the bay region. Cation $9^+$ also crystallized from acetone in a triclinic system with space group $P\bar{1}$ (see Table S5 and Figure S7 in the Supporting Information) as a racemic mixture of the possible enantiomers, P and M. Due to its fjord region, $9^+$ exhibits a helical geometry with a torsion angle of 28.579°.

Meanwhile, the synthesis of $5^+$ was achieved using a slightly modified literature procedure (see the Experimental Section for


DOI: 10.1021/jacs.5b07959
J. Am. Chem. Soc. 2015, 137, 14944−14951

details),[37] resulting in crystals of $5^+$ as the tetrafluoroborate salt that proved suitable for X-ray diffraction. Analysis of the resulting X-ray structure of $5^+$ (see Table S6 and Figure S5 in the Supporting Information) shows an arrangement in a triclinic system, with antiplanar $\pi$-stacking interactions giving rise to two parallel columns in the unit cell. Between these columns, antiplanar $\pi-\pi$ interacting pairs of $5^+$ are arranged with a separation of 3.367−3.393 Å. The molecule can be considered planar with negligibly small torsion angles of 1.067° and 0.525° in the bay regions. Illustrations of the assembly of $5^+$, $8^+$, and $9^+$ obtained from X-ray structure analysis are displayed below in Figure 2.

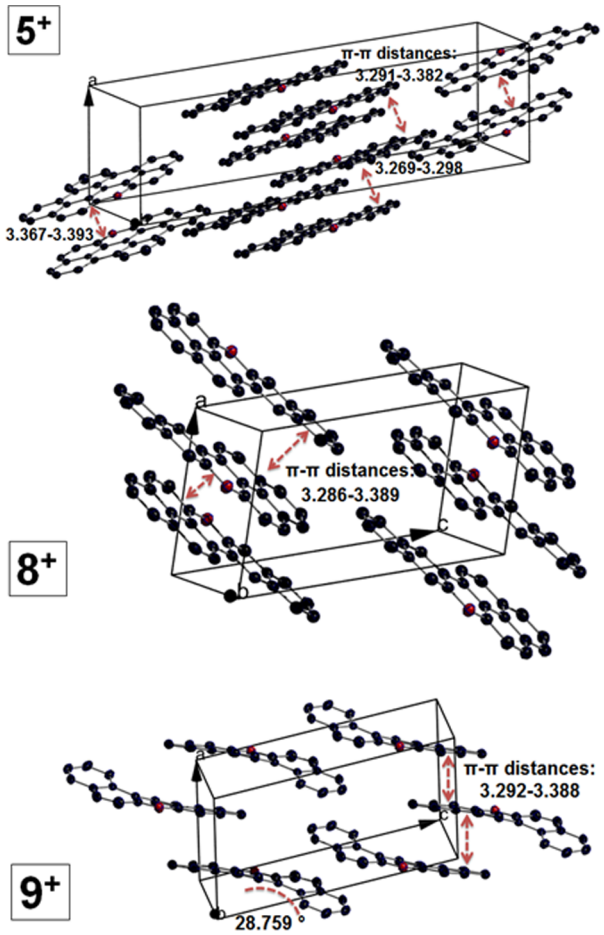


**Figure 2.** Illustration of $\pi-\pi$ stacking arrangements of compounds $5^+$, $8^+$, and $9^+$ obtained from X-ray structure analysis. Counterions are not displayed for clarity.

In terms of electronic properties, cation $8^+$ shows a red shift of 13 nm in its absorption spectrum compared with the previously reported cation $4^+$ on account of the more extended polyaromatic framework in $8^+$ (Figure 3). The same trend is also evident with $9^+$, but to an even greater extent. $9^+$ shows a broader absorption than $8^+$ with a maximum at 505 nm (a bathochromic shift of 36 nm compared with $8^+$). This result is unexpected and intriguing, given that the benzene-fused skeleton is less linear in $9^+$ than it is in $8^+$. According to Clar's approach, $9^+$ comprises more Robinson rings than $8^+$, and hence, $9^+$ should exhibit a higher aromaticity when compared to $8^+$. This in turn would imply that $9^+$ should absorb shorter wavelengths of light than $8^+$. However, as this is clearly

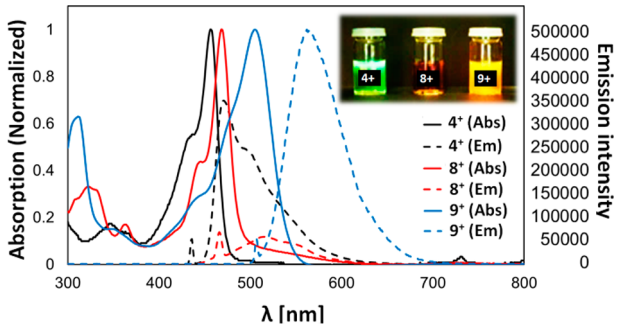


**Figure 3.** UV−vis and fluorescence spectra of $4^+$, $8^+$, and $9^+$ in MeCN.

not the case, we propose that the geometry and the position of the pyrylium ring in $9^+$ disrupt this aromaticity and cause a bathochromic shift to manifest instead.

The different intensities of fluorescence emission from $4^+$, $8^+$, and $9^+$ could be observed with the naked eye (Figure 3, inset). The fluorescence emission spectra (Figure 3) show the emission of $4^+$ ($2.8 \times 10^{-5}$ mol/L), $8^+$ ($1 \times 10^{-5}$ mol/L), and $9^+$ ($3.1 \times 10^{-6}$ mol/L) upon excitation at 435, 465, and 505 nm, respectively. $4^+$ emits between 450 and 600 nm with a maximum at 471 nm, giving a Stokes shift of 15 nm. $8^+$ also emits up to 600 nm, however with a considerably lower intensity. The maximum peak lies at 516 nm, which corresponds to a Stokes shift of 47 nm. A broad emission between 510 and 690 nm can be observed for $9^+$ with a maximum peak at 562 nm, indicating a red shift (and a higher intensity) compared with $8^+$. Cation $8^+$ displayed a relatively low intensity compared to $4^+$ and $9^+$. This can be attributed to collisional quenching by $\pi-\pi$ stacking interactions. In the case of $9^+$, the helical structure results in the minimization of $\pi-\pi$ interactions and hence a greater emission intensity.

The cyclic voltammogram of $8^+$ is shown as the black dashed line in Figure 4 (see the Supporting Information for electrochemical methods). Two reversible redox waves are evident centered around −0.43 and −1.53 V vs ferrocene/ferrocenium. The less negative of these waves corresponds to the formation of the neutral radical species, and the second to the formation of the $8^-$ monoanion. A cyclic voltammogram of $9^+$ under the same conditions is shown for comparison as a

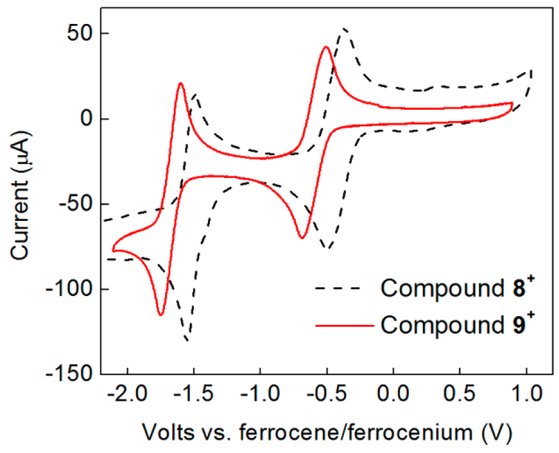


**Figure 4.** Cyclic voltammograms of $8^+$ and $9^+$ at room temperature obtained at a scan rate of 100 mV $s^{-1}$ on a glassy carbon working electrode of area 0.071 $cm^{-2}$. Peaks are referenced to the $Fc/Fc^+$ couple (wave not shown).



DOI: 10.1021/jacs.5b07959
J. Am. Chem. Soc. 2015, 137, 14944−14951

solid red line in Figure 4. Again, two well-defined reversible waves are evident in the absence of oxygen, occurring at roughly −0.59 and −1.67 V vs ferrocene/ferrocenium. Compared to $4^+$,[35] these redox processes for $8^+$ are both somewhat less negative. In the case of $4^+$, $E_{cation/radical} = -0.52$ V for the formation of the neutral radical from the cation, while the reduction of this radical to give the anion occurred at $E_{radical/anion} = -1.66$ V. This indicates that $8^+$ is easier to reduce than $4^+$, in both the cationic and neutral radical forms, possibly on account of the greater degree of delocalization in $8^+$. For $9^+$, formation of the neutral radical species is harder than in the case of $4^+$, but formation of the cation occurs at roughly the same potential. In contrast, compound $5^+$ showed significantly more cathodic shifts for both its corresponding waves with $E_{cation/radical} = -0.96$ V and $E_{radical/anion} = -1.80$ V (see Figure S1 in the Supporting Information).

When cyclic voltammograms of $8^+$ and $9^+$ were recorded under an air atmosphere, the first redox waves for both compounds (corresponding to the cation/radical redox processes) showed very good reversibility, which is indicative of a lack of side reactions. After 2000 cycles at a scan rate of 100 mV/s, no depletion of the first redox wave for either $8^+$ or $9^+$ was observed (Figure 5). These results could be reproduced

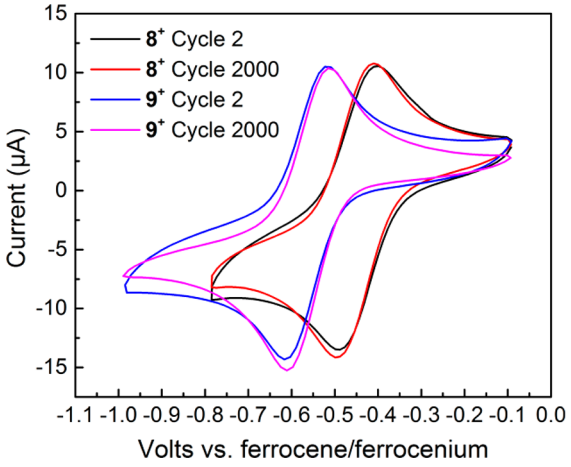


**Figure 5.** Cyclic voltammograms of compounds $8^+$ and $9^+$ at room temperature and under an air atmosphere at a scan rate of 100 mV $s^{-1}$ on a glassy carbon electrode of area 0.071 $cm^2$. Peaks are referenced to the $Fc/Fc^+$ couple. Both compounds were cycled 2000 times.

using the same samples after 1 week. Hence, radicals **8** and **9** may be capable of acting as stable paramagnetic redox partners without the need for an inert atmosphere. These radicals are stable to redox cycling in air, with no significant degradation evident by cyclic voltammetry (CV) over the course of several hours. Other radicals (e.g., DPPH, TEMPO, and verdazyl radicals) are also stable over long periods of time. However, in these cases, the spin density is concentrated on heteroatoms (O and N) and bulky substituents are required to prevent deleterious side reactions from occurring. This is in contrast to the carbon-based, delocalized radicals stabilized through electronics that we report herein. The second redox waves for both **8** and **9** (corresponding to the radical/anion redox couples) were found to be irreversible when probed under air.

The radicals **8** and **9** were formed electrochemically by bulk electrolysis of solutions of the corresponding cations at −1.0 V vs ferrocene/ferrocenium with 0.1 M $N(Bu)_4BF_4$ as the supporting electrolyte. Upon complete reduction to the radicals, the color of the solutions had turned to yellow and dark red for **8** and **9**, respectively. The UV/vis spectra showed the full depletion of the absorption peaks indicative of the cations and suggested the presence of the corresponding radicals (see Figure S2 in the Supporting Information). In the case of **8**, three maxima were detected with values at 403, 441, and 465 nm, as well as a shoulder at 494 nm. Further absorption peaks were evident between 300 and 380 nm with peaks at 320, 335, and 362 nm which appear to be similar to the absorption of the corresponding cation. The UV spectrum of **9** shows strong absorption between 320 and 450 nm with a clear maximum peak at 360 nm. Furthermore, a broad shoulder with moderate absorption can be found between 455 and 565 nm. It is noteworthy that the absorption spectrum of radical **9** is very similar to the absorption spectrum of radical **4** published previously.[35]

Product solutions from completed bulk electrolyses were investigated by EPR spectroscopy, which confirmed that radicals had been formed. Signals with $g$ values of 2.00258 and 2.0028 were obtained for **8** and **9**, respectively, which are close to that of a free electron ($g$ = 2.002319). Figure 6 shows

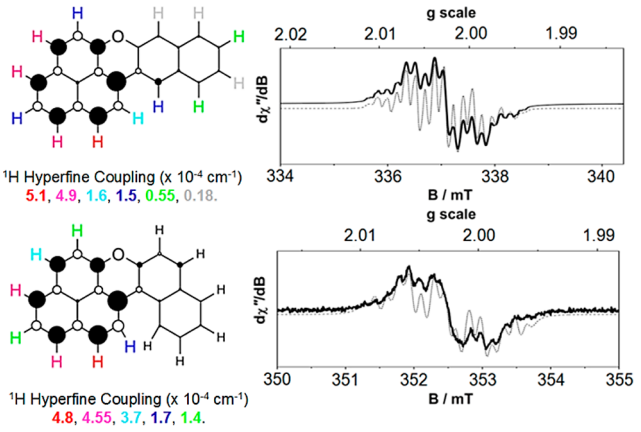


**Figure 6.** X-band EPR spectra of **8** and **9** in DMSO at 293 K. Experimental conditions for **8**: frequency, 9.4481 GHz; power, 0.63 mW; modulation, 0.02 mT. Experimental conditions for **9**: frequency, 9.8812 GHz; power, 0.63 mW; modulation, 0.02 mT. Experimental data are shown by the black traces and the simulations as gray lines.

the coupling patterns in which the total number of lines, hypothetically made up of $(2 \times 1 \times 1/2 + 1)^{13} = 8192$ lines, cannot be observed due to the limited resolution. Nonetheless, by computational methods Mulliken spin densities (calculated at the M05-2X/6-31G** level of theory; see Tables S2 and S3 in the Supporting Information) could be assigned to the radical centers. These spin densities correlate with the hyperfine coupling constants, allowing spectra which match with the experimental spectra to be simulated (see Figure 6, and Figures S3 and S4 in the Supporting Information). It is noteworthy that the spin densities at the $\alpha$-position of the phenalenyl skeleton are below the corresponding spin densities of 1,9-dithiophenalenyl (**3**) (0.51 and 0.54 mT),[28,29] indicative of a higher stabilization of **8** and **9** compared with **3**.

Using the bond lengths obtained from the X-ray data, harmonic oscillating model of aromaticity (HOMA)[43] indices were calculated using the HOMA model formula.[44] In addition, nucleus independent chemical shift (NICS)[45] values of dummy atoms centered 1 Å above the plane of benzenoid rings were computed on the basis of the B3LYP level of theory using the


DOI: 10.1021/jacs.5b07959
J. Am. Chem. Soc. 2015, 137, 14944−14951

6-31+G* basis set. For compound $5^+$, the pyrylium ring exhibits the lowest HOMA and NICS values of 0.42 and −4.21 due to the perturbation caused by the oxygen atom (see Figure 7).

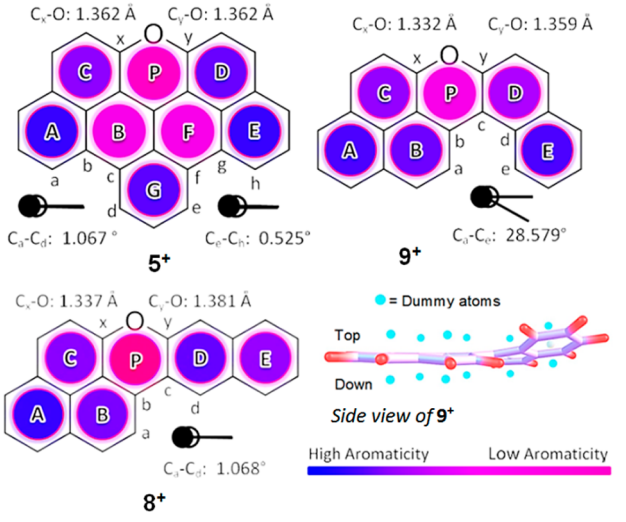


**Figure 7.** Molecular structures of $5^+$, $8^+$, and $9^+$ showing C−O distances and torsion angles in the bay and fjord regions. HOMA values are calculated using bond lengths from X-ray data analysis. NICS values are obtained from calculation based on the B3LYP level of theory using the 6-31+G* basis set. In the case of $9^+$, the NICS values for both sides of the molecule were computed using dummy atoms which are 1 Å from the center of each ring.

The bond lengths of $C_x$−O and $C_y$−O are identical (1.362 Å). The degrees of aromaticity for the inner rings B and F are distinctly lower compared to those of the outer rings (see Table S1 in the Supporting Information). Rings A, E, and G exhibit the highest degrees of aromaticity. The inner rings are less aromatic than rings C and D; hence, $5^+$ appears to comprise two naphthalene substructures at the outer frames (A−C and D−E) characterized by their electronic structure. Thus, there appears to be less phenalenyl character in $5^+$ than in $8^+$ or $9^+$, which could explain the more cathodic reduction potentials of $5^+$ relative to $8^+$ and $9^+$ (less phenalenyl character and so less stabilization through delocalization).

The evaluation of the aromaticity for $8^+$ shows that the three rings A, B, and C resemble more the electronic structure of phenalenyl than is the case for $5^+$. The naphthalene unit annulated with the pyrylium ring has a slightly higher degree of aromaticity in ring D compared to ring E. It is noteworthy that the $C_x$−O bond is distinctly shorter than the $C_y$−O bond, indicating that a nucleophile (e.g., hydroxide) would not be prone to attack the ring at the $C_y$ position. This is consistent with Clar's rule, as otherwise a loss of aromaticity would result, which can be depicted by depletion of one Robinson ring. The tendency for a nucleophilic attack at the $C_x$ and $C_b$ positions is additionally decreased due to the conjugation provided by the phenalenyl unit, resulting in an optimal stabilization of the whole molecule.

As $9^+$ is nonplanar, a statement about the aromaticity based on the electromagnetic parameters using NICS values is considered for both sides of the plane at a distance of 1 Å from the center of each six-membered ring. The pyrylium ring exhibits a slight enhancement of aromaticity compared with the ones for $8^+$ and $5^+$, which is observed by considering the HOMA index and NICS values of 0.52 and −5.93/−7.22, respectively. Contrary to $8^+$, the benzene ring E in $9^+$ is more aromatic than ring D adjacent to the pyrylium ring. Comparing the planarities of the pyrylium rings in all the presented molecules, the root-mean-square deviations of fitted atoms in these rings are below 0.01 Å, indicating a negligible geometrical effect on the degrees of aromaticity.

We propose that a more pronounced oxonium−carbenium resonance structure is found on the side of the phenalenyl unit in cations $8^+$ and $9^+$ (when compared to cation $5^+$) represented by the bond lengths of 1.337 and 1.332 Å, respectively. Hence, it appears that cations $8^+$ and $9^+$ have the propensity to resemble the electronic structure of the chromophore compound phenalenone.[46] In contrast, $5^+$ shows very low degrees of aromaticity in the inner rings B and F. Thus, a delocalization pattern similar to a phenalenyl unit comparable with $8^+$ and $9^+$ is nonexistent; i.e., $5^+$ can be classified as a non-phenalenyl-type cation. This aromaticity evaluation may indicate that compounds $8^+$ and $9^+$ do not represent typical electronic structures of xanthenyl species due to the presence of the phenalenyl skeleton. In contrast with xanthenyl, $8^+$ and $9^+$ are not prone to undergo nucleophilic attack on the 4-position of the pyrylium ring. Hence, we demonstrate that a phenalenyl unit combined with pyrylium derivatives can result in complementary electronic systems, where the two $\alpha$-positions of the phenalenyl moiety represent the common reactive sites of the pyrylium ring (the 2′ and 4′ positions). Such a situation was previously suggested by Haddon and co-workers as a result of their elegant work with 1,9-dithiophenalenyl (**3**), which incorporates a 1,2-dithiolyl ring.[28,29] However, we note that the oxidized forms of the phenalenyl radicals presented herein also represent fascinating dyes and hence may also open up new avenues of research in the area of phenalenyl chemistry.

## CONCLUSIONS

In conclusion, we have demonstrated that our synthetic protocol gives access to a new series of $\pi$-amphoteric species of interest in the field of phenalenyl chemistry, including the first example of a helical phenalenyl radical stabilized only by the incorporation of a heteroatom ever reported. Our results highlight the remarkable stability of these electronically stabilized radicals, which can be stored under air for weeks without noticeable degradation. It is noteworthy that phenalenyl and pyrylium species on their own give short-lived radicals upon one-electron reduction under air, which subsequently undergo side reactions such as $\sigma$-dimerization. Hence, the high reversibility of the cation-radical redox processes under air reported herein suggests an intriguing complementary stabilization between the phenalenyl and pyrylium substructures, affording novel, stable phenalenyl-type species which may act as dyes or stable open-shell species depending on their redox states. Although $8^+$ and $9^+$ have an electronic structure based on phenalenyl (in contrast to $5^+$), the overall polyaromatic frameworks of these two compounds represent two distinct scaffolds due to their differing shapes. Interestingly, the absorption of $9^+$ is distinctly red-shifted compared with that of $8^+$ despite its less linear benzene-fused skeleton. The nonplanar topology of $9^+$ prevents efficient fluorescence quenching by $\pi$−$\pi$ interactions compared with its isomer $8^+$. This, in combination with its water solubility, makes $9^+$ a promising candidate as a dye for DNA intercalation studies. Future work in our laboratory will endeavor to focus on the potential applications of these compounds and on preparing


DOI: 10.1021/jacs.5b07959
J. Am. Chem. Soc. 2015, 137, 14944−14951

even more complex and topologically interesting cations and radicals of this sort.

## ■ ASSOCIATED CONTENT

### Supporting Information

The Supporting Information is available free of charge on the ACS Publications website at DOI: 10.1021/jacs.5b07959.

X-ray crystallographic data for $9^+$ (CIF)
X-ray crystallographic data for $8^+$ (CIF)
X-ray crystallographic data for $5^+$ (CIF)
Detailed experimental protocols, additional electrochemical, electronic, EPR, computational, and crystallographic data, and characterization of all new compounds reported herein (PDF)

## ■ AUTHOR INFORMATION


### Corresponding Author

*goebu@chem.gla.ac.uk


### Notes

The authors declare no competing financial interest.

## ■ ACKNOWLEDGMENTS

M.D.S. thanks the University of Glasgow for a Kelvin Smith Research Fellowship. This work was supported by the University of Glasgow and the Engineering and Physical Sciences Research Council (EPSRC). L.C. thanks the Royal Society for a Wolfson Merit Award. L.C. would like to thank the EPSRC for funding (Grants EP/J015156/1, EP/K021966/1, EP/K023004/1, EP/L015668/1, EP/L023652/1), and the EC project 318671 MICREAGENTS).

## ■ REFERENCES


(1) Reid, D. H. *Q. Rev., Chem. Soc.* **1965**, *19*, 274−302.
(2) Sun, Z.; Wu, J. *J. Mater. Chem.* **2012**, *22*, 4151−4160.
(3) Bosson, J.; Gouin, J.; Lacour, J. *Chem. Soc. Rev.* **2014**, *43*, 2824−2840.
(4) Herse, C.; Bas, D.; Krebs, F. C.; Bürgi, T.; Weber, J.; Wesolowski, T.; Laursen, B. W.; Lacour, J. *Angew. Chem., Int. Ed.* **2003**, *42*, 3162−3166.
(5) O'Connor, G. D.; Troy, T. P.; Roberts, D. A.; Chalyavi, N.; Fückel, B.; Crossley, M. J.; Nauta, K.; Stanton, J. F.; Schmidt, T. W. *J. Am. Chem. Soc.* **2011**, *133*, 14554−14557.
(6) Mukherjee, A.; Sen, T. K.; Ghorai, P.; Mandal, S. K. *Sci. Rep.* **2013**, *3*, 2821.
(7) Small, D.; Zaitsev, V.; Jung, Y.; Rosokha, S. V.; Head-Gordon, M.; Kochi, J. K. *J. Am. Chem. Soc.* **2004**, *126*, 13850−13858.
(8) Kuratsu, M.; Kozaki, M.; Okada, K. *Angew. Chem., Int. Ed.* **2005**, *44*, 4056−4058.
(9) Cyrański, M. K.; Havenith, R. W. A.; Dobrowolski, M. A.; Gray, B. R.; Krygowski, T. M.; Fowler, P. W.; Jenneskens, L. W. *Chem. - Eur. J.* **2007**, *13*, 2201−2207.
(10) McLachlan, A. D. *Mol. Phys.* **1960**, *3*, 233−252.
(11) Martin, J. C.; Smith, R. G. *J. Am. Chem. Soc.* **1964**, *86*, 2252−2256.
(12) Bowie, W. T.; Feldman, M. R. *J. Am. Chem. Soc.* **1977**, *99*, 4721−4726.
(13) Faldt, A.; Krebs, F. C.; Thorup, N. *J. Chem. Soc., Perkin Trans. 2* **1997**, 2219−2228.
(14) Sørensen, T. J.; Laursen, B. W. *J. Org. Chem.* **2010**, *75*, 6182−6190.
(15) Laursen, B. W.; Sørensen, T. J. *J. Org. Chem.* **2009**, *74*, 3183−3185.
(16) Nicolas, C.; Lacour, J. *Org. Lett.* **2006**, *8*, 4343−4346.
(17) Sen, T. K.; Mukherjee, A.; Modak, A.; Ghorai, P.; Kratzert, D.; Granitzka, M.; Stalke, D.; Mandal, S. K. *Chem. - Eur. J.* **2012**, *18*, 54−58.
(18) Krebs, F. C.; Spanggaard, H.; Rozlosnik, N.; Larsen, N. B.; Jørgensen, M. *Langmuir* **2003**, *19*, 7873−7880.
(19) Pariyar, A.; Vijaykumar, G.; Bhunia, M.; Dey, S. Kr.; Singh, S. K.; Kurungot, S.; Mandal, S. K. *J. Am. Chem. Soc.* **2015**, *137*, 5955−5960.
(20) Chi, X.; Itkis, M. E.; Reed, R. W.; Oakley, R. T.; Cordes, A. W.; Haddon, R. C. *J. Phys. Chem. B* **2002**, *106*, 8278−8287.
(21) Morita, Y.; Miyazaki, E.; Yokoyama, T.; Kubo, T.; Mochizuki, E.; Kai, Y.; Nakasuji, K. *Synth. Met.* **2003**, *135−136*, 617−618.
(22) Itkis, M. E.; Chi, X.; Cordes, A. W.; Haddon, R. C. *Science* **2002**, *296*, 1443−1445.
(23) Urdampilleta, M.; Klyatskaya, S.; Cleuziou, J.-P.; Ruben, M.; Wernsdorfer, W. *Nat. Mater.* **2011**, *10*, 502−506.
(24) Sanvito, S. *Nat. Mater.* **2011**, *10*, 484−485.
(25) Reynisson, J.; Schuster, G. B.; Howerton, S. B.; Williams, L. D.; Barnett, R. N.; Cleveland, C. L.; Landman, U.; Harrit, N.; Chaires, J. B. *J. Am. Chem. Soc.* **2003**, *125*, 2072−2083.
(26) Pothukuchy, A.; Mazzitelli, C. L.; Rodriguez, M. L.; Tuesuwan, B.; Salazar, M.; Brodbelt, J. S.; Kerwin, S. M. *Biochemistry* **2005**, *44*, 2163−2172.
(27) Morita, Y.; Suzuki, S.; Sato, K.; Takui, T. *Nat. Chem.* **2011**, *3*, 197−204.
(28) Haddon, R. C.; Wudl, F.; Kaplan, M. L.; Marshall, J. H.; Cais, R. E.; Bramwell, F. B. *J. Am. Chem. Soc.* **1978**, *100*, 7629−7633.
(29) Beer, L.; Mandal, S. K.; Reed, R. W.; Oakley, R. T.; Tham, F. S.; Donnadieu, B.; Haddon, R. C. *Cryst. Growth Des.* **2007**, *7*, 802−809.
(30) Suzuki, S.; Morita, Y.; Fukui, K.; Sato, K.; Shiomi, D.; Takui, T.; Nakasuji, K. *J. Am. Chem. Soc.* **2006**, *128*, 2530−2531.
(31) Sabacky, M. J.; Johnson, C. S., Jr.; Smith, R. G.; Gutowsky, H. S.; Martin, J. C. *J. Am. Chem. Soc.* **1967**, *89*, 2054−2058.
(32) Bowie, W. T.; Feldman, M. R. *J. Am. Chem. Soc.* **1977**, *99*, 4721−4726.
(33) Torricelli, F.; Bosson, J.; Besnard, C.; Chekini, M.; Bürgi, T.; Lacour, J. *Angew. Chem., Int. Ed.* **2013**, *52*, 1796−1800.
(34) Ueda, A.; Wasa, H.; Suzuki, S.; Okada, K.; Sato, K.; Takui, T.; Morita, Y. *Angew. Chem., Int. Ed.* **2012**, *51*, 6691−6695.
(35) Anamimoghadam, O.; Symes, M. D.; Busche, C.; Long, D.-L.; Caldwell, S. T.; Flors, C.; Nonell, S.; Cronin, L.; Bucher, G. *Org. Lett.* **2013**, *15*, 2970−2973.
(36) Kubo, T.; Katada, Y.; Shimizu, A.; Hirao, Y.; Sato, K.; Takui, T.; Uruichi, M.; Yakushi, K.; Haddon, R. C. *J. Am. Chem. Soc.* **2011**, *133*, 14240−14243.
(37) Wu, D.; Pisula, W.; Haberecht, M. C.; Feng, X.; Müllen, K. *Org. Lett.* **2009**, *11*, 5686−5689.
(38) Frisch, M. J.; Trucks, G. W.; Schlegel, H. B.; Scuseria, G. E.; Robb, M. A.; Cheeseman, J. R.; Scalmani, G.; Barone, V.; Mennucci, B.; Petersson, G. A.; Nakatsuji, H.; Caricato, M.; Li, X.; Hratchian, H. P.; Izmaylov, A. F.; Bloino, J.; Zheng, G.; Sonnenberg, J. L.; Hada, M.; Ehara, M.; Toyota, K.; Fukuda, R.; Hasegawa, J.; Ishida, M.; Nakajima, T.; Honda, Y.; Kitao, O.; Nakai, H.; Vreven, T.; Montgomery, J. A., Jr.; Peralta, J. E.; Ogliaro, F.; Bearpark, M.; Heyd, J. J.; Brothers, E.; Kudin, K. N.; Staroverov, V. N.; Kobayashi, R.; Normand, J.; Raghavachari, K.; Rendell, A.; Burant, J. C.; Iyengar, S. S.; Tomasi, J.; Cossi, M.; Rega, N.; Millam, J. M.; Klene, M.; Knox, J. E.; Cross, J. B.; Bakken, V.; Adamo, C.; Jaramillo, J.; Gomperts, R.; Stratmann, R. E.; Yazyev, O.; Austin, A. J.; Cammi, R.; Pomelli, C.; Ochterski, J. W.; Martin, R. L.; Morokuma, K.; Zakrzewski, V. G.; Voth, G. A.; Salvador, P.; Dannenberg, J. J.; Dapprich, S.; Daniels, A. D.; Farkas, Ö.; Foresman, J. B.; Ortiz, J. V.; Cioslowski, J.; Fox, D. J. *Gaussian 09*, revision D.01; Gaussian, Inc.: Wallingford, CT, 2009.
(39) Becke, A. D. *J. Chem. Phys.* **1993**, *98*, 5648−5652.
(40) Zhao, Y.; Schultz, N. E.; Truhlar, D. G. *J. Chem. Theory Comput.* **2006**, *2*, 364−382.
(41) Ditchfield, R.; Hehre, W. J.; Pople, J. A. *J. Chem. Phys.* **1971**, *54*, 724−728.
(42) Koelsch, C. F.; Anthes, J. A. *J. Org. Chem.* **1941**, *6*, 558−565.




DOI: 10.1021/jacs.5b07959
J. Am. Chem. Soc. 2015, 137, 14944−14951

(43) Kruszewski, J.; Krygowski, T. M. *Tetrahedron Lett.* **1972**, *13*, 3839−3842.
(44) Krygowski, T. M. *J. Chem. Inf. Model.* **1993**, *33*, 70−78.
(45) Schleyer, P. R.; Maerker, C.; Dransfeld, A.; Jiao, H.; Hommes, N. J. R. v. E. *J. Am. Chem. Soc.* **1996**, *118*, 6317−6318.
(46) Daza, M. C.; Doerr, M.; Salzmann, S.; Marian, C. M.; Thiel, W. *Phys. Chem. Chem. Phys.* **2009**, *11*, 1688−1696.



DOI: 10.1021/jacs.5b07959
*J. Am. Chem. Soc.* 2015, 137, 14944−14951